LA-UR- 11-06199

Approved for public release; distribution is unlimited.

Title: A Figure of Merit for Radiographic Performance Based on Contrast-to-Noise Ratio

Author(s):
C. Tomkins (P-21)
F. Merrill (P-25)
S. Watson (N-2)
T. Haines (P-23)
C. Morris (P-25)

Intended for: Report for Headquarters

Los Alamos
NATIONAL LABORATORY
EST. 1943

Los Alamos National Laboratory, an affirmative action/equal opportunity employer, is operated by the Los Alamos National Security, LLC for the National Nuclear Security Administration of the U.S. Department of Energy under contract DE-AC52-06NA25396. By acceptance of this article, the publisher recognizes that the U.S. Government retains a nonexclusive, royalty-free license to publish or reproduce the published form of this contribution, or to allow others to do so, for U.S. Government purposes. Los Alamos National Laboratory requests that the publisher identify this article as work performed under the auspices of the U.S. Department of Energy. Los Alamos National Laboratory strongly supports academic freedom and a researcher's right to publish; as an institution, however, the Laboratory does not endorse the viewpoint of a publication or guarantee its technical correctness.

Form 836 (7/06)

A Figure of Merit for Radiographic Performance Based on Contrast-to-Noise Ratio

LA-UR 11-0xxxx

C. Tomkins (P-21), F. Merrill (P-25), S. Watson (N-2),
T. Haines (P-23), C. Morris (P-25)

Los Alamos National Laboratory

October 27, 2011

1. Introduction

Defining radiographic performance in a meaningful way for a range of technologies and requirements is a challenging task. Two key elements of performance are the ability to measure density (or transmission), and the ability to resolve an edge or feature. The former task is the main focus of this paper, owing to its inherent complexity, although the latter is also discussed. Our goal here is to outline an appropriate Figure of Merit (FOM) that may be used to inform decisions with respect to radiographic capabilities at the NNSS. We will also attempt to communicate relevant caveats and context, as appropriate.

To this end, we first discuss various sources of error in NNSA radiography, and review which sources of error are impacted by the choice of radiographic system (below, in Section 1). A figure of merit is then introduced that uses the Contrast-to-Noise ratio, CNR, to identify the object-thickness regimes that are "optimum" based on the mean free path ($\lambda = 1/\mu$) of the particle type (Section 2). This figure of merit is then applied in the task of measuring a relative pathlength difference of 1% for a range of object thicknesses. For both x-rays and protons, we demonstrate the number of particles required to perform this discrimination task with 99% confidence (Section 3). The ability to resolve an edge or feature is discussed in Section 4. This task depends on several factors, but is addressed here by the dominant factor in most applications, the spatial resolution of the system. One straightforward way of quantifying spatial resolution is introduced. Finally, and for completeness, several important considerations outside the scope of this FOM are briefly discussed.

Sources of error in NNSA radiography

Typically, the underlying goal in attempting to develop a figure of merit (FOM) is to gain an understanding of how well we will be able to measure a quantity of interest. In NNSA radiography, this quantity is often density, ρ, and we would like to know how well we can measure density in a given experiment (or set of experiments) for different candidate radiographic systems (machines & detectors). It is thus instructive to examine the sources of error in radiographic experiments of interest to NNSA. An expression for error in density, ε_ρ, is given below in Eqn 1.

$$\epsilon_\rho = \sqrt{\epsilon_{poisson}^2 + \epsilon_{noise}^2 + \epsilon_{blur}^2 + \epsilon_{scatter}^2 + \epsilon_{coll}^2 + \epsilon_{overlying}^2 + \epsilon_{3D}^2 + \epsilon_{sys}^2} \qquad \text{Equation 1}$$

Here the sources of error are assumed to be uncorrelated, which may not be strictly true in all cases but is reasonable for the present purpose. Subscripts denote the sources of error as follows: *poisson*, for uncertainty due to particle statistics; *noise*, for all non-particle-counting sources of noise, such as noise sources in the camera system; *blur*, for errors due to all

potential sources of blur; *scatter*, representing all sources of scatter, uncorrelated and correlated with the direct signal; *coll*, representing errors associated with graded or other collimation, or misalignment of such; *overlying*, representing errors associated with overlying materials in the radiographic line of sight; *3D*, representing three-dimensional effects; and *sys*, intended to capture all other systematic sources of error not mentioned explicitly elsewhere. Note that other sources of error exist, and this expression will change based on the specifics of a given experiment—but this is one reasonable way of writing such an expression, and it is intended to be broadly applicable within the context of NNSS radiography.

We are now able to examine this equation when asking the critical question, "How well will we be able to measure density?" The answer, of course, depends not only on the radiographic source and detector, but also the experiment. Importantly, the radiographic source will directly impact the first term, $\varepsilon_{poisson}$, the third term, ε_{blur}, and may impact the fourth term, $\varepsilon_{scatter}$. The source will not have a strong impact on other terms, however, particularly those associated with systematic errors. Hence, *the extent to which a Figure of Merit is an appropriate measure of our ability to estimate density depends heavily on the relative magnitudes of the terms in Equation 1.* For regimes in which particle statistics are a dominant source of error, which might be the case for thicker objects, a FOM that captures these effects will be highly relevant. For regimes in which particle statistics are a small or negligible source of error relative to other terms, which might be the case for thinner objects, such an FOM will no longer be as relevant in terms of performance on real experiments. For example, reducing poisson noise to some fraction of other error sources might be good enough for a given measurement; moreover, further reduction in this one term may not yield overall improvement in the measurement, as suggested by an improving FOM. The relevance of an FOM in intermediate regimes will vary, of course, as the relative magnitudes of these error terms shift. Hence, ultimate decisions on radiographic systems should be informed not only by particle statistics errors but also by systematic and other errors for experiments of interest.

Despite these caveats, characterization of radiographic systems remains a critical part of understanding total error. Moreover, in the complex task of selecting a radiographic source, an FOM remains a critical tool in that it allows for comparison of certain fundamental effects that are broadly present in radiographic measurement.

2. A figure of merit for transmission measurement: CNR

It is a common task in radiography to quantitatively measure differential pathlength[1] as illustrated in Figure 1. Given this task, one might ask the following questions. First, assuming a fixed dose and a fixed differential pathlength, how confident are we that the measured

[1] Sometimes called Line-Of-Sight mass, or Areal Mass, or Area Density.

difference is real; i.e. what is the constrast sensitivity of our measurement? A second, related question is: what diagnostic dose, or alternatively how many particles, is required to establish a high level of confidence about a hypothetical pathlength difference from a differential absorption measurement?

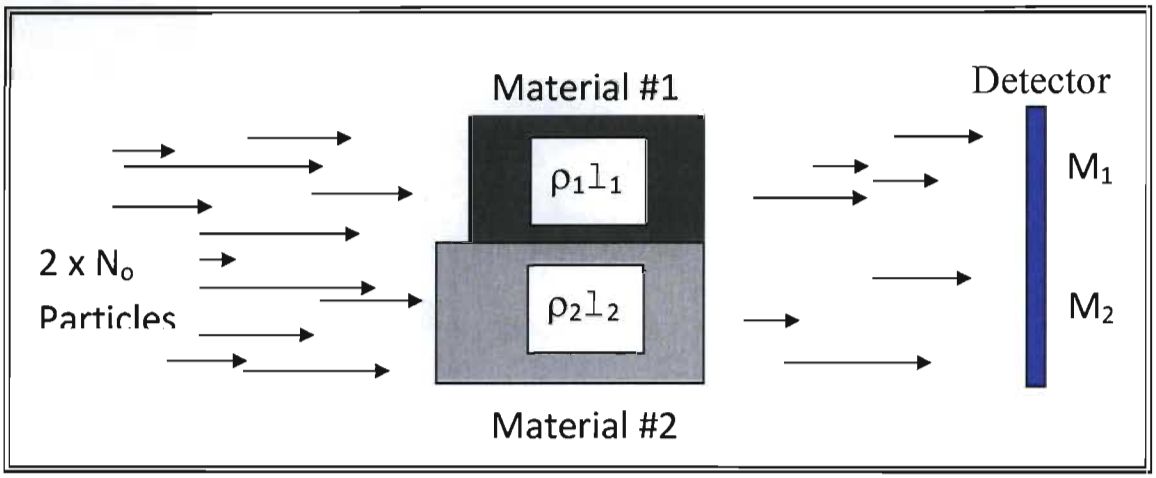

Figure 1 – Differential Absorption Measurement of Two Slabs of Material

We start with a basic model based upon Beer's law as shown in Figure 1. In this model, the total mass absorption coefficient, μ/ρ, is assumed to be constant with respect to particle energy and absorber material. This model assumption is only strictly true for mono-energetic, isotopic sources. Further, material #1 must be the same composition, but not necessarily the same density, as material #2. In general, these requirements are rarely met in practice. However, for megavolt radiography, the mass energy absorption coefficient is approximately constant over a wide range of energy and material Z. Thus, for the sake of this analysis, we can say that these conditions are approximately satisfied for certain applications.

Let us establish two measurements. The first measurement, M_1, is simply a transmission measurement of N_o incident particles absorbed in a material with pathlength $\rho_1\ell_1$. The second, nearly identical measurement, M_2, has the same conditions as the first except applied to a different material pathlength, $\rho_2\ell_2$as follows:

$$M_1 = N_o \exp\left(-\frac{\mu}{\rho}\rho_1\ell_1\right)$$

Equation 2

$$M_2 = N_o \exp\left(-\frac{\mu}{\rho}\rho_2\ell_2\right)$$

Equation 3

Our ability to measure this difference will come from the system with the largest difference in transmission relative to the noise in the measurement. Figure 2 demonstrates this effect.

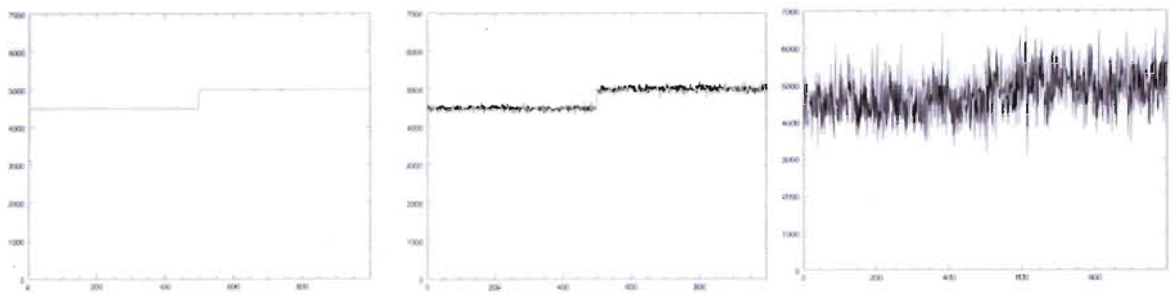

Figure 2: (left) The thickness of an object has a step change in the center of the field of view and the extent of this step change needs to be measured. (middle) A low noise system allows a high fidelity measurement of this step change. (right) a high noise system will not measure this density as well. A useful figure of merit will result in the choice of the middle result over the right result.

We will return to Eqns 2 and 3 in the next Section when we make statistical statements about our ability to discriminate between these 2 objects for given particles. Here we introduce the figure of merit. The above type of measurement is typical in the imaging world and contrast-to-noise ratio is commonly used as a figure of merit to characterize the imaging systems. This figure of merit for radiography applications is shown in equation 1, where the contrast to noise ratio is related to the detected transmission.

$$CNR = \frac{\Delta N_D / \sqrt{N_D}}{\Delta l / l} = \frac{l}{\sqrt{N_D}} \frac{dN_D}{dl} = l \sqrt{\frac{N_0}{T_D}} \frac{dT_D}{dl} \qquad \text{Equation 4}$$

In equation 4, *CNR* is the contrast to noise ratio, normalized to fractional object thickness $\Delta l/l$, N_D is the detected probes and T_D is the detected transmission. It is important to note that these are detected quantities. By requiring detected quantities we are able to include detection efficiency in this FOM. If scatter background or long-range blur are significant contributors to the detected transmission, these quantities could be included in the evaluation of this FOM. This will most likely require simulations rather than an analytic evaluation of equation 4.

It is useful to view this FOM for the most familiar as well as simplest analysis of x-ray radiography. In this analysis Beer's law, which is shown in a simplified form (assume $\mu = 1$) in Eqn. 5, is assumed for detected transmission measurement.

$$T = e^{(-l)} \qquad \text{Equation 5}$$

This figure of merit is the classic CNR per fractional object thickness. Therefore, this CNR multiplied by the expected fractional change in object thickness provides an estimate of the contrast to noise ratio for this change in object thickness. Note that one must specify a desired spatial resolution or length scale in order to calculate this FOM. The resolution comes into this calculation through N_D, which will be determined by the (resolution)^2 through the particle density flux at the detector. This specified length scale might be a nominal value, such as 1 mm, to make comparisons on a uniform per-mm^2 basis. Or, this length scale might be determined from the fundamental resolution of the radiography system. One reasonable way to define this is to use the FWHM values discussed in Section 4.

Example FOM Calculation

In this example the object thickness, *l*, is measured in units of mass attenuation lengths (also referred to interaction lengths). With the simplifying assumptions of 100% detection efficiency and no scatter background the FOM is easily determined analytically. This result is shown in Equation 6.

$$CNR_{Beer} = l\sqrt{N_o}e^{-l/2} \qquad \text{Equation 6}$$

This provides the familiar result that the FOM improves as the square root of the number of particles. The CNR analysis also yields the result that the maximum of the FOM occurs when l=2 interaction lengths. A curve of this FOM for a pure beer's law attenuation radiography system is shown in figure 3.

This simple example shows that this FOM has the attractive properties of going to zero at 100% transmission and going to zero at 0% transmission, and peaking somewhere in between.

The above FOM gives important information in terms of where in the object-thickness regime a given particle type is "optimum" by the CNR criteria, where it is off-peak but relatively strong, and where it is relatively weak. It would be informative to link such an analysis to absolute performance, which is the goal of the following Section.

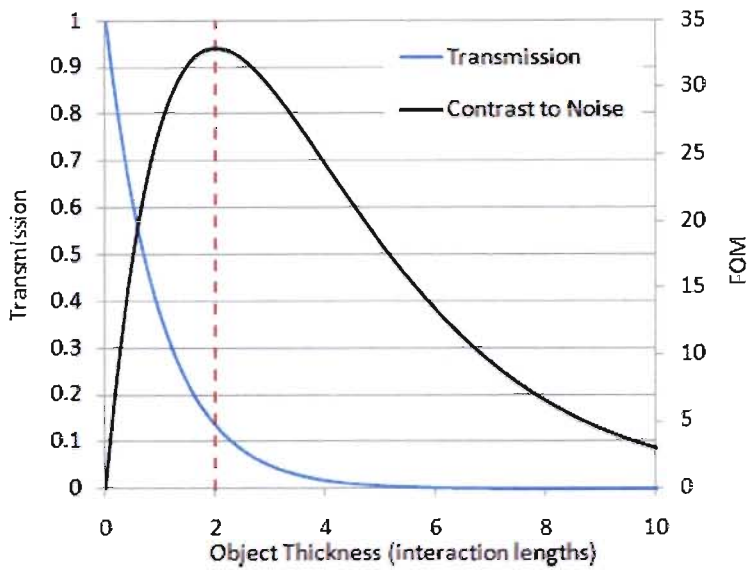

Figure 3: Beer's law attenuation is shown by the transmission curve. The figure of merit described in equation 6 is also shown. This FOM peaks with the object thickness at twice the interaction length (mass attenuation coefficient for x-rays).

3. Application of FOM to estimate measurement error

In this section, we link the concepts in the above FOM to absolute performance, such as the ability of a radiographic system to measure to within some error the thickness difference in the simple problem described earlier. This problem may also be formulated by asking how many incident particles are required per unit area to achieve a given measurement accuracy. To do this, we return to Eqns 2 and 3, following on from their definitions, assuming x-rays, and using their notation.

We define a differential absorption measurement, ΔM:

$$\Delta M = M_1 - M_2 = N_o\left[\exp\left(-\frac{\mu}{\rho}\rho_1\ell_1\right) - \exp\left(-\frac{\mu}{\rho}\rho_2\ell_2\right)\right] \qquad \text{Equation 7}$$

Because the two measurements, M_1 and M_2, are independent, the standard measurement error on their difference, $\sigma_{\Delta M}$, is given by the following[i]:

$$\sigma_{\Delta M} = \sqrt{\sigma_{M_1}^2 + \sigma_{M_2}^2} \qquad \text{Equation 8}$$

$$\sigma_{M_1} = \sqrt{M_1}\,, \sigma_{M_2} = \sqrt{M_2} \qquad \text{Equation 9}$$

$$\sigma_{\Delta M} = \sqrt{M_1 + M_2} = \sqrt{N_o\left[\exp\left(-\frac{\mu}{\rho}\rho_1\ell_1\right) + \exp\left(-\frac{\mu}{\rho}\rho_2\ell_2\right)\right]} \qquad \text{Equation 10}$$

The task we are interested in here is to determine if this measured difference is statistically different from zero and if so, with what degree of confidence. To do this, we must compare the expected difference, ΔM, with the standard error, $\sigma_{\Delta M}$, for a given confidence level, α. For α = 0.90 (i.e. 90% confidence), $\Delta M > 1.30\sigma_{\Delta M}$; similarly for α =0.95, $\Delta M > 1.65\sigma_{\Delta M}$; and for α =0.99, $\Delta M > 2.33\sigma_{\Delta M}$. Utilizing these constraints and solving for the number of particles, N_o, required we obtain the following boundary condition.

$$N_o \geq \frac{1.3^2\left[\exp\left(-\frac{\mu}{\rho}\rho_1\ell_1\right) + \exp\left(-\frac{\mu}{\rho}\rho_2\ell_2\right)\right]}{\left[\exp\left(-\frac{\mu}{\rho}\rho_1\ell_1\right) - \exp\left(-\frac{\mu}{\rho}\rho_2\ell_2\right)\right]^2} \qquad \text{for } \alpha = 0.90 \qquad (7)$$

The results of this boundary condition are plotted in Figure 4 for the case of a fixed (Δl=1g/cm^2) pathlength difference. Note that for varying object thickness l, a constant pathlength difference Δl gives *varying* normalized contrast $\Delta l/l$, which was the basis of the FOM. Similar results are plotted in Figure 5 for the case of a fractional (1%) pathlength difference, $\Delta l/l$ = 0.01, which is obviously a constant within the CNR formulation. Both plots assume μ/ρ = 0.045cm^2/g, which is typical for megavolt radiography.

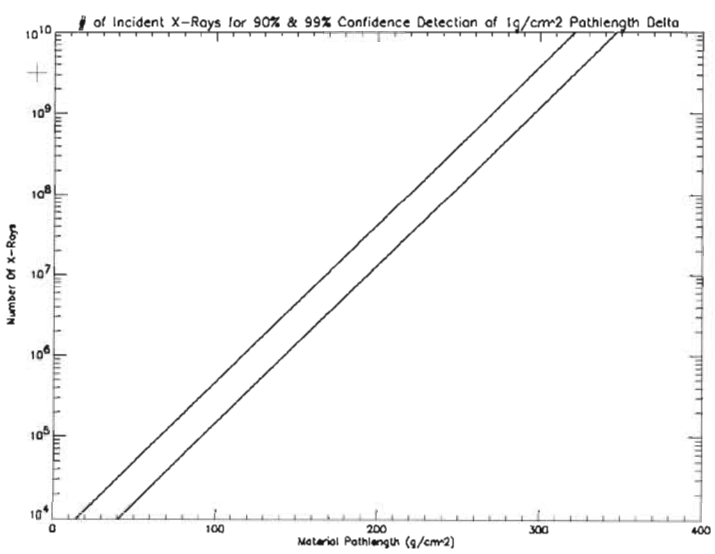

Figure 4 – Incident X-Rays (μ/ρ = 0.045) Required To Discern *Absolute* (1g/cm^2) Pathlength Differences With (90% & 99%) Confidence vs. Total Material Pathlength

Note that the number of particles necessary to achieve a statistically significant result in Figure 5 has a clear minimum, indicating an optimal pathlength for maximum statistical contrast. This is the same fundamental behavior captured by the (peaked) FOM earlier. The key question, of course, is whether or not a given radiographic system yields measurement errors that are acceptable given the system requirements, regardless of the distance from the "optimum" value. This must be determined for each radiographic system, experiment, and set of requirements considered.

In general, one would like the *shortest* pathlength that allows enough particles through for the desired accuracy on the most opaque features. Even this rule must be balanced against practical considerations like detector dynamic range, and background effects (e.g. visible light scatter, signal bias etc.)

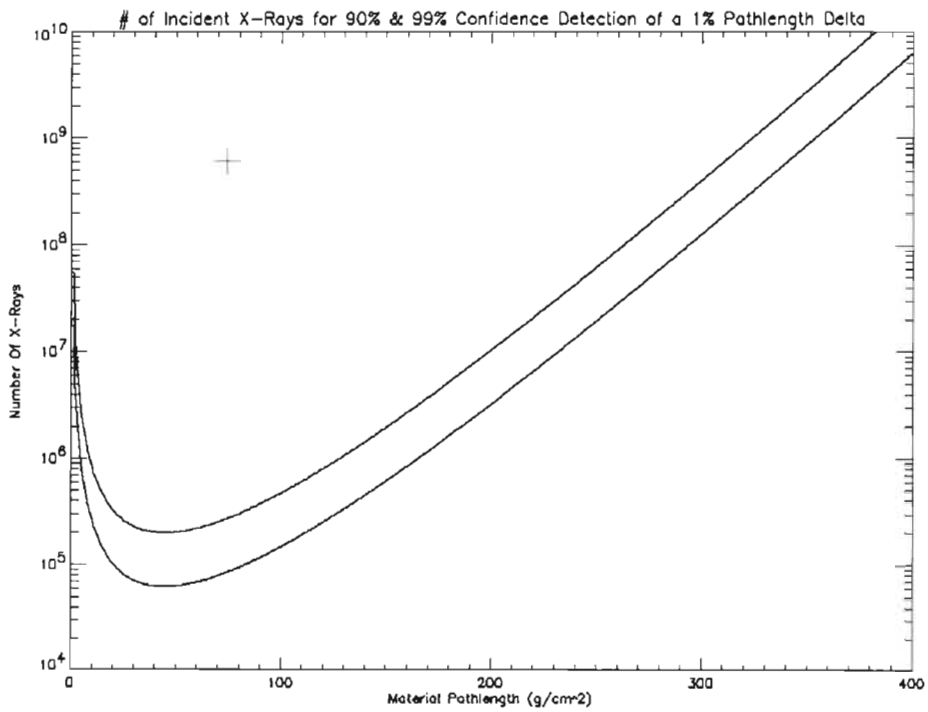

Figure 5 – Incident X-Rays (μ/ρ = 0.045) Required to Discern a 1% *Fractional* Pathlength Difference With (90% & 99%) Confidence vs. Total Pathlength (ρ l).

Trends for X-rays and Protons

We have thus established the number of x-ray particles required to achieve a given level of sensitivity as a function of object pathlength. We might then ask, how many particles are actually available in a typical geometry for a DARHT-like X-ray machine? Figure 6 illustrates the number of γ-rays (>1MeV) per Rad-cm^2 as a function of electron energy for a range of energies commonly used for penetrating radiography. It is worth noting that because the below figures are on a per Rad-cm^2 basis, converting them to an actual error (or directly relating them to the particle requirements in Figure 5) requires knowledge or assumptions of experimental geometry, desired spatial resolution, and machine dose.

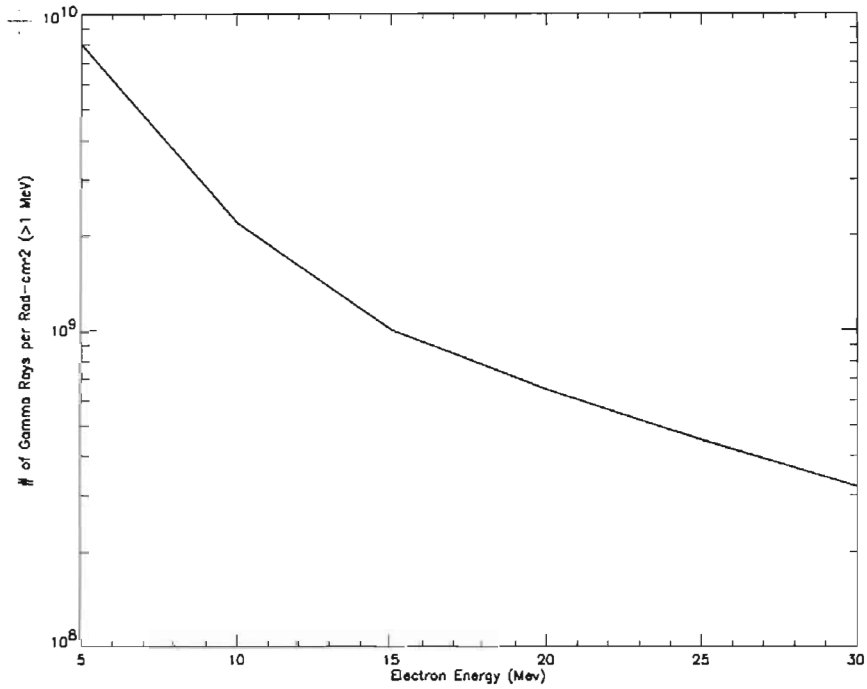

Figure 6 – Number of γ-rays (>1MeV) per Rad-cm^2 vs Electron Energy[2]

We may also calculate the number of protons required for these characteristic tasks as a function of pathlength. Figure 7 illustrates the number of particles of both types necessary to accomplish a detection of 1% fractional pathlength change in uranium, and Figure 8 illustrates the case of a fixed (1g/cm^2) pathlength difference. From Figure 7, which most directly relates to our CNR, we observe that <u>a large number of protons are necessary to discern differences in thinner objects, and a large number of γ-rays are necessary to penetrate thicker objects.</u>

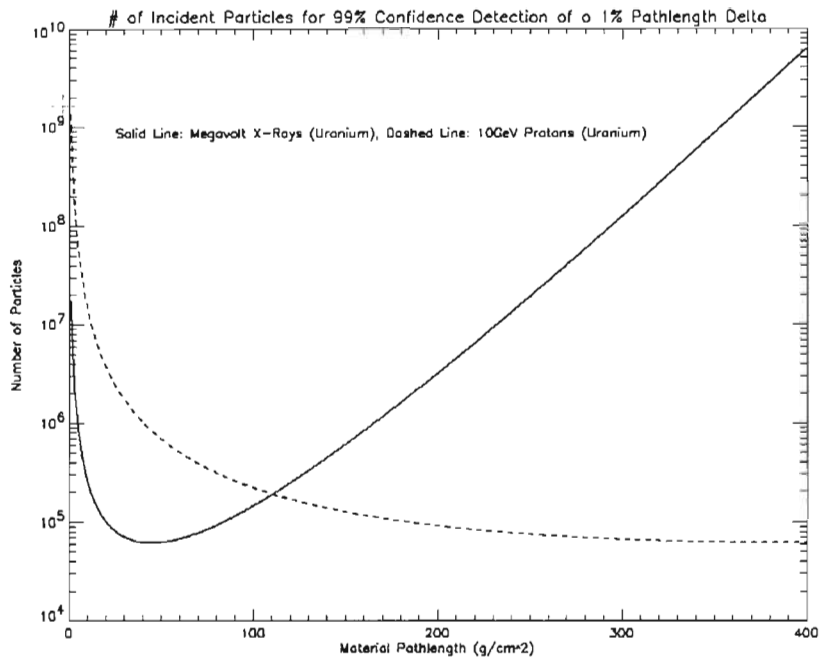

Figure 7 – γ-Rays and 10 GeV Protons Necessary for a 1% Fractional Pathlength Discrimination Task (α=0.99).

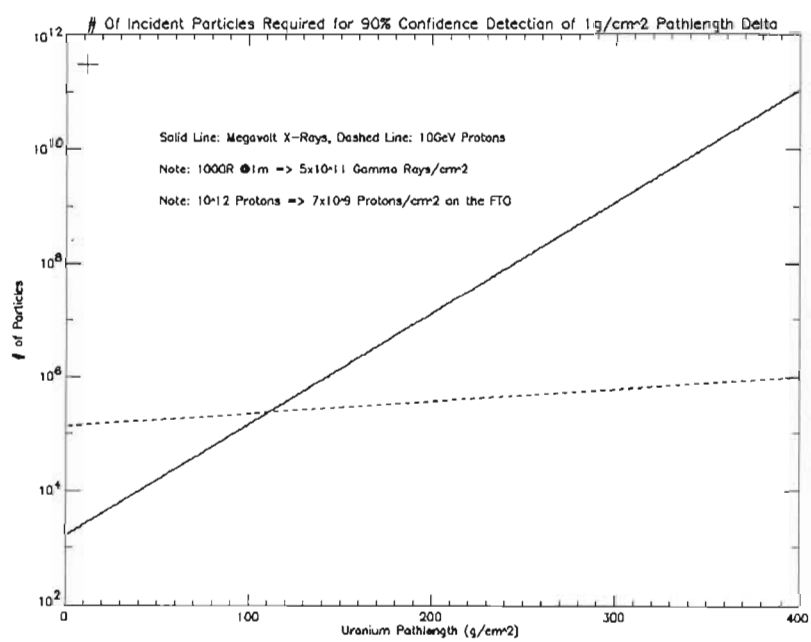

Figure 8 – γ-Rays and 10Gev Protons necessary for a 1g/cm^2 Fixed Pathlength Discrimination Task (α=0.90).

4. Quantification of spatial resolution

To allow us to properly capture the relative strengths and weaknesses of different radiographic systems, we consider separately the characterization of the resolution of the radiographic system. Although we reiterate that a single number cannot fully characterize the resolution function of any imaging system, we recognize that finding a single representative number is required here. We propose to use the full-width at half-maximum of the system line spread function (LSF), which is the derivative of the edge spread function (ESF). This can be estimated by considering the radiograph that generates an extended step function in the measured transmission. Such a step function is typically measured by radiographing a rolled-edge, which is least susceptible to misalignment issues. A high statistics measure of the system resolution can be measured by integrating along the edge to generate a one-dimensional graph of the transmission across the edge (this is the ESF). An example of this technique is shown in figure 9, which is a measurement of the 800 MeV proton radiography system at LANL. Proton radiography sources typically have a Gaussian point spread function; therefore, the measured edge transition was fit to the edge transition that is expected from a Gaussian edge spread function. In fact, the specification for the shape of the blur function, along with the FWHM, fully characterizes the resolution of the imaging modality, provided that the specification of the shape is exactly correct (and aside from effects that are difficult to measure via the edge spread function, but can occur, such as low intensity long range components to the blur function). These effects may also arise through a spatially-correlated scatter background. Some sources can have processes with very-long-range effects, so that objects far outside the field of view scatter probes back into the field of view. These effects are best characterized through their effects on density resolution.

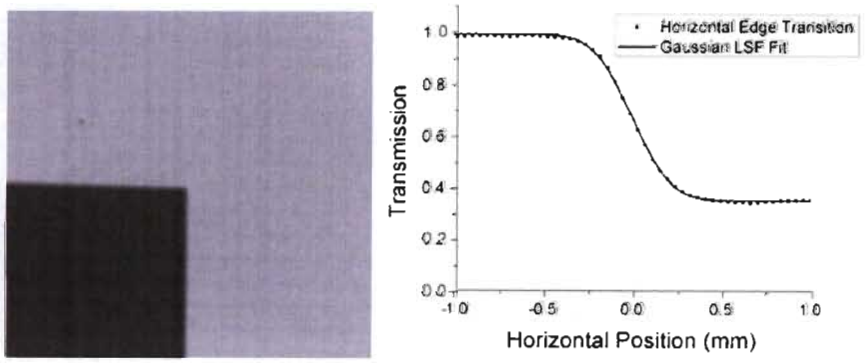

Figure 1: (left) An 800 MeV proton radiograph of a 6 mm thick tungsten edge, which has been precision aligned to be perpendicular to the incident proton beam. A square edge allows the simultaneous measurement of the horizontal and vertical resolution in a single radiograph. An average over the vertical edge has been used to generate a high statistics measure of the transmission step across this edge. (Note curve is actually ESF, not LSF).

5. Additional Characteristics of Radiographic Imaging Systems

There are other important characteristics beyond those discussed here that must be considered when identifying the appropriate radiographic source. Temporal resolution of a single pulse is often an important quantity, which is easily characterized by the radiation pulse duration. Some applications also require or would greatly benefit from fast measurements at multiple times, so this is another consideration. Another characteristic that is typically overlooked is the operational repetition rate of the pulsed source. Data collected for characterization and calibration of the source and system are often as important as the dynamic object radiographs. Sources can be more fully optimized and characterized if measurements can be made quickly and at small expense—and these results can impact measurement error on the dynamic event. Finally, repeatability of the source is an important characteristic. With advanced analysis techniques, increasingly accurate measurements are possible through modeling different effects, but this is done most accurately with a repeatable source (so that the static object data is truly representative of the dynamic data).

6. Conclusions

Methods of evaluating radiographic imaging systems are discussed. Emphasis is placed on one general task in radiography: the ability to quantitatively measure a relative difference in pathlength. We derive a Figure of Merit (FOM) based upon the contrast-to-noise ratio (CNR) for such a task, and show how this FOM can be used to illuminate areas of relative strength and weakness in pathlength space for given particles. This FOM is then linked to system performance requirements for a specific $\Delta l/l$ by examining how many particles are required to achieve a 1% fractional measurement with a given confidence. This is done for both x-rays and protons as a function of object pathlength. It shown that fewer x-rays are required for thinner objects, and fewer protons are required for thicker objects. The methodology also provides a framework for evaluation of candidate radiographic systems, given dose, experimental geometry, desired spatial resolution, and desired accuracy. We also outline one approach to defining system spatial resolution, the FWHM of the LSF. Finally, a general expression for density errors in NNSA radiography is discussed. Populating the terms in such an expression for a given class of experiments can provide important insights into when the sources of error captured by the FOM are highly relevant, moderately relevant, or less relevant in determining quantities of interest.

Notes

This paper is an attempt at combining separate, existing pieces of work into a coherent document. Frank Merrill's (P-25) "A common figure of merit for the comparison of radiographic imaging modalities" was heavily used in Sections 2 and 4. Scott Watson's (N-2) "Contrast Sensitivity in Radiography: the Princess and the Pea" was heavily used in Section 3, and also used in Section 2. References are found in those documents.